Solid State Communications 249 (2017) 48–53

Contents lists available at ScienceDirect

Solid State Communications

journal homepage: www.elsevier.com/locate/ssc

Communication

# The collision frequency model of the solid state plasma for $Si/Si_{1-x}Ge_x/Si$ SPiN device

H.Y. Kang*, H.Y. Hu, B. Wang, H.M. Zhang, H. Su, M.R. Hao

*Key Laboratory for Wide Band-Gap Semiconductor Materials and Devices, School of Microelectronics, Xidian University, Xi'an 710071, People's Republic of China*

ARTICLE INFO

*Keywords:*
A.Solid state plasma
D.Collision frequency
D.Heterojunctions

ABSTRACT

A two dimensional(2D) collision frequency model is developed based on the 2D solid state plasma concentration distribution model and mobility model for a heterogeneous $Si/Si_{1-x}Ge_x/Si$ structure SPiN(Surface PiN) devices, which are the basic radiating elements in the reconfigurable solid state plasma antenna. The lower collision frequency can be achieved when the Ge mole fraction x and applied voltage increase at the temperature T=300 K, and that the basically uniform distribution of collision frequency can be obtained for Ge mole fraction x=0.3. Moreover, radiation efficiency and the maximum gain of the antenna for the different collision frequency have also been studied. The proposed model can be a handful for the designing of the solid state plasma antenna.

## 1. Introduction

Silicon-based solid state plasma antenna is characterized by wide radiation range, good stealth characteristic, compatible with microelectronic technology and dynamic reconfiguration, etc. So far, Si/Si/Si SPiN devices are used as the basic radiating elements in the reconfigurable solid state plasma antenna [1–4]. However, the drawback is that the solid state plasma concentration in the intrinsic region(I-region) is low, which limits the performance of the antenna. Hence, a heterogeneous $Si/Si_{1-x}Ge_x/Si$ structure SPiN device, which is shown in Fig. 1, is proposed to improve the solid state plasma concentration. $Si_{1-x}Ge_x$ is a semiconductor alloy material, its properties can be changed by adjusting the Ge mole fraction x [5–7]. The mobility of the electron and hole in the $Si_{1-x}Ge_x$ alloy is higher than that of Si. Due to the lower barrier potential, $Si/Si_{1-x}Ge_x/Si$ SPiN device is more effective to improve the injection ratio than the Si/Si/Si SPiN device.

The collision frequency is the critical parameter of solid state plasma which influence the maximum gain and the radiation efficiency of the antenna [8]. According to the literature [9,10], the collision frequency is assumed as a constant in HFSS simulation, but that as a function of concentration must be nonuniform due to the nonuniform concentration distribution. Consequently, the performance of antenna simulated must have a large error from the actual value. But little has been done in this regard so far.

In this paper, we have proposed an effective solid state plasma collision frequency model within the I-region based on the $Si/Si_{1-x}Ge_x/Si$ heterogeneous SPiN device. The model is developed by the 2D solid state plasma concentration distribution model and mobility model. The purposes of this model were, first, to study how does the collision frequency distributed within the I-region, second, to investigate the trend of the collision frequency with the Ge mole fraction x, applied voltage and the temperature, third, to verify the effect of the collision frequency on the antenna. Finally, uniform collision frequency distribution can be obtained under the optimized parameters. The proposed model can provide a theoretical basis for the designing of the solid state plasma antenna.

## 2. Two dimensional concentration distribution model of solid state plasma

Under steady state forward bias operation, the solid state plasma concentration will form a steady two dimensional distribution within the I-region of the SPiN device. Setting the length direction is L-axis and the depth direction is D-axis, as shown in Fig. 2. In order to simplify the model, it is essential to make the following assumptions:

(1) Quasi charge neutral condition $[n(l, d) = p(l, d)]$ is valid at each point of the I-region.
(2) Supposing that the transport of the plasma diffuse along the L-axis firstly, then, setting the L-axis as a starting point, diffuse along the D-axis.

* Corresponding author.
*E-mail address:* kanghaiyan5200@163.com (H.Y. Kang).

http://dx.doi.org/10.1016/j.ssc.2016.11.001
Received 4 July 2016; Received in revised form 2 November 2016; Accepted 4 November 2016
Available online 07 November 2016
0038-1098/

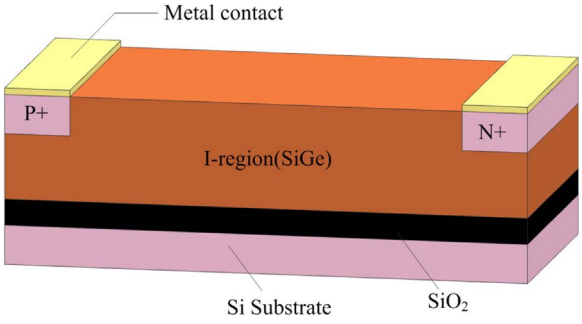


**Fig. 1.** The structure of SPiN device.

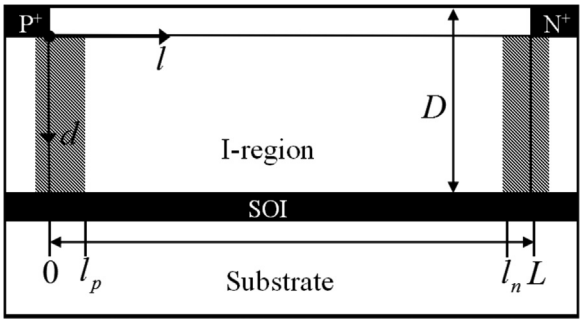


**Fig. 2.** The vertical profile of the SPiN device.

At a given depth d, the solid state plasma concentration along the L-axis has a distribution of catenary form with just two exponential basis functions [11], as shown in Eq. (1). However, at a given $l$, downward diffusion of the plasma is accompanied by a recombination process that leads to an exponential decay of the plasma concentration along the D-axis, as shown in Eq. (2):

$$n(l) = A\exp\left(\frac{l}{L_a}\right) + B\exp\left(-\frac{l}{L_a}\right) \quad (0 \le l \le L) \tag{1}$$

$$n(d) = C\exp\left(-\frac{d}{L_a}\right) \quad (0 \le d \le D) \tag{2}$$

where $L_a$ is the diffusion length given by $L_a = \sqrt{D_a\tau}$, $D_a$ is given by $D_a = 2D_nD_p/(D_n + D_p)$, $D_n$ and $D_p$ are the electron and hole diffusion coefficients, respectively. $\tau$ is the diffusion lifetime within the I-region. A, B and C are arbitrary constants determined by boundary conditions at the Pi/Ni junctions and the surface concentration of the SPiN device.

The coefficients in Eq. (1) and Eq. (2) are obtained by using the following boundary conditions by Fletcher [12].

i) At the $Si/Si_{1-x}Ge_xPi$ heterojunction interface $l = l_p$, solid state plasma concentration is described as,

$$n(l_p) = \frac{\gamma_1(m_{op} + m_{oi}\gamma_1)}{1 - \gamma_1^2} \tag{3}$$

ii) At the $Si_{1-x}Ge_x/SiNi$ heterojunction interface $l = l_n$, solid state plasma concentration is given by,

$$n(l_n) = \frac{\gamma_2(m_{on} + m_{oi}\gamma_2)}{1 - \gamma_2^2} \tag{4}$$

iii) At the surface layer of the I-region, the solid state plasma concentration can be written as,

$$n(d)|_{d=0} = n(l) \tag{5}$$

where $m_{op}$, $m_{on}$ and $m_{oi}$ are equilibrium majority plasma concentration in the $P^+$ region, $N^+$ region and I-region, respectively, defined by

$$m_{op} = N_A - \frac{n_{i(Si)}^2}{N_A},\ m_{oi} = N_d - \frac{n_{i(SiGe)}^2}{N_d},\ m_{on} = N_D - \frac{n_{i(Si)}^2}{N_D} \tag{6}$$

$\gamma_1$ and $\gamma_2$ are given by

$$\gamma_1 = \exp[q(V_{Pi} - V_{D1})/kT],\ \gamma_2 = \exp[q(V_{Ni} - V_{D2})/kT] \tag{7}$$

where $V_{Pi}$ and $V_{Ni}$ is the applied forward bias voltage drop of the Pi and Ni heterojunction, respectively.$V_{D1}$ and $V_{D2}$ is the barrier potential of the Pi and Ni heterojunction, respectively. $n_{i(Si)}$ and $n_{i(SiGe)}$ is the intrinsic carrier concentration of the Si and SiGe.$N_A$, $N_d$ and $N_D$ denote doping concentration of the $P^+$ region , the I-region and the $N^+$ region, respectively. $q$ is the electronic charge, $k$ is a Boltzmann's constant, $T$is the temperature.

Thus, the coefficients A, B and C can be given as:

$$\begin{cases} A = \dfrac{\gamma_1 N_A \exp\left(-\frac{l_n}{L_a}\right) - \gamma_2 N_D \exp\left(-\frac{l_p}{L_a}\right)}{\exp\left(-\frac{l_n - l_p}{L_a}\right) - \exp\left(\frac{l_n - l_p}{L_a}\right)} \\ B = \dfrac{\gamma_1 N_A \exp\left(\frac{l_n}{L_a}\right) - \gamma_2 N_D \exp\left(\frac{l_p}{L_a}\right)}{\exp\left(\frac{l_n - l_p}{L_a}\right) - \exp\left(-\frac{l_n - l_p}{L_a}\right)} \\ C = \dfrac{\gamma_1 N_A \exp\left(\frac{l - l_n}{L_a}\right) - \gamma_2 N_D \exp\left(\frac{l - l_p}{L_a}\right)}{\exp\left(-\frac{l_n - l_p}{L_a}\right) - \exp\left(\frac{l_n - l_p}{L_a}\right)} + \dfrac{\gamma_1 N_A \exp\left(\frac{l_n - l}{L_a}\right) - \gamma_2 N_D \exp\left(\frac{l_p - l}{L_a}\right)}{\exp\left(\frac{l_n - l_p}{L_a}\right) - \exp\left(-\frac{l_n - l_p}{L_a}\right)} \end{cases} \tag{8}$$

where

$$l_p = \sqrt{\frac{2\varepsilon_0\varepsilon_{SiGe}V_{D1}}{qN_d}},\ l_n = L - \sqrt{\frac{2\varepsilon_0\varepsilon_{SiGe}V_{D2}}{qN_d}} \tag{9}$$

where$\varepsilon_0$is the permittivity of vacuum, $\varepsilon_{SiGe}$ is the permittivity of the $Si_{1-x}Ge_x$, which is defined by $\varepsilon_{SiGe} = 11.7 + 4.1x$.

Substituting the Eq. (8) into the Eq. (1) and Eq. (2), the 2D concentration distribution model of the solid state plasma within the I-region can be written as

$$\begin{aligned} n(l, d) = {} & \frac{\gamma_1 N_A \exp\left(-\frac{l_n}{L_a}\right) - \gamma_2 N_D \exp\left(-\frac{l_p}{L_a}\right)}{\exp\left(-\frac{l_n - l_p}{L_a}\right) - \exp\left(\frac{l_n - l_p}{L_a}\right)} \exp\left(\frac{l - d}{L_a}\right) \\ & + \frac{\gamma_1 N_A \exp\left(\frac{l_n}{L_a}\right) - \gamma_2 N_D \exp\left(\frac{l_p}{L_a}\right)}{\exp\left(\frac{l_n - l_p}{L_a}\right) - \exp\left(-\frac{l_n - l_p}{L_a}\right)} \exp\left(-\frac{l + d}{L_a}\right) \end{aligned}$$

$$(0 \le l \le L,\ 0 \le d \le D) \tag{10}$$

where

$$\begin{cases} \gamma_1 = \exp\left[\frac{1}{kT}(qV_{Pi} - \Delta E_C - \frac{1}{2}(E_{g(Si)} - 0.487x)) - \log\left(\frac{N_A n_{i(SiGe)}}{N_d n_{i(Si)}}\right)\right] \\ \gamma_2 = \exp\left[\frac{1}{kT}(qV_{Ni} + \Delta E_C - \frac{1}{2}(E_{g(Si)} - 0.487x)) - \log\left(\frac{N_d n_{i(Si)}}{N_D n_{i(SiGe)}}\right)\right] \end{cases} \tag{11}$$

According to the current continuity equations, the junction voltages $V_{Pi}$ and $V_{Ni}$ can be obtained as

$$\begin{cases} V_{Pi} = \frac{1}{2}\left[V + \frac{kT}{q}\ln\left[\frac{1}{\beta}\frac{N_D D_n \exp\left(\frac{l_n - l_p}{L_a}\right) + D_n N_D \exp\left[\frac{l_p - l_n}{L_a}\right] - 2N_D D_p}{2N_A D_n - N_A D_p \exp\left[\frac{l_p - l_n}{L_a}\right] - N_A D_p \exp\left(\frac{l_n - l_p}{L_a}\right)}\right]\right] \\ V_{Ni} = \frac{1}{2}\left[V - \frac{kT}{q}\ln\left[\frac{1}{\beta}\frac{N_D D_n \exp\left(\frac{l_n - l_p}{L_a}\right) + D_n N_D \exp\left[\frac{l_p - l_n}{L_a}\right] - 2N_D D_p}{2N_A D_n - N_A D_p \exp\left[\frac{l_p - l_n}{L_a}\right] - N_A D_p \exp\left(\frac{l_n - l_p}{L_a}\right)}\right]\right] \end{cases} \tag{12}$$

where $\beta$ is defined by $\beta = \exp[q(V_{D2} - V_{D1})/kT]$, V is the applied voltage.

## 3. Two dimensional collision frequency model of solid state plasma

Collision frequency is a key parameter in the designing of the antenna, which will influence the radiation efficiency and the maximum gain of the antenna. The model of the collision frequency can be obtained based on the mobility model, the relationship between the collision frequency and the mobility can be expressed as [13]:

$$\nu = \frac{e}{m\mu} \tag{13}$$

where $\nu$ is the collision frequency, $\mu$ is the mobility, $m$ is conductivity effective mass, e is the electronic charge.

The mobility of the solid state plasma in the I-region for the Si/$Si_{1-x}Ge_x$/Si SPiN device is influenced by multiple scattering mechanisms, such as acoustic phonons scattering [14], carrier-carrier scattering [15], alloy scattering [16] and ionized impurity scattering, etc. According to the Masetti model [17], the ionized impurity scattering effect is small at room temperature for the doping concentration below $10^{16}$ $cm^{-3}$. The I-region of the SPiN device we discussed above is lightly doped with $10^{14}$ $cm^{-3}$, so impurity scattering can be ignored in the following discussion.

Assuming that the various scattering mechanisms are independent of the mobility, the use of Matthiessen's rule to calculate the total mobility is valid, which is given by

$$\mu^{-1} = \mu_{alloy}^{-1} + \mu_{phonon}^{-1} + \mu_{np}^{-1} + \mu_{other}^{-1} \tag{14}$$

where

$$\mu_{alloy} = \frac{16e\hbar^3 T^{-1/2}}{3m_{xy}^2 \Omega_0 S(a) V_{alloy}^2 x(1-x)} \left(\frac{33m_z e^2 n(l,d)}{8\varepsilon_{SiGe}\hbar^2}\right)^{-1/3} \tag{15}$$

$$\mu_{phonon} = \mu_L \left(\frac{T}{300}\right)^{-\xi} \tag{16}$$

$$\mu_{np} = \frac{D(T/300)^{3/2}}{n(l,d)} \left[\ln\left(1 + F\left(\frac{T}{300}\right)^2 n(l,d)^{-2/3}\right)\right]^{-1} \tag{17}$$

where $\mu_{alloy}$ is alloy scattering mobility, $\mu_{phonon}$ is acoustical phonons scattering mobility, $\mu_{np}$ is carrier-carrier scattering mobility, $\mu_{other}$ is the mobility limited by ionized impurity scattering and all other scattering mechanisms, which can be neglected. $\Omega_0$ is the atomic volume, $\hbar$ is the Planck's constant. $V_{alloy}$ is the alloy disorder potential, for electron and hole, $V_{alloy}$ is different. $S(a)$ is an energy dependent parameter, if the material is completely random, we assume that $S(a) = 1$.$m_{xy}$ and $m_z$ are the transverse and longitudinal effective mass of the electron, we use $m_{xy} = (0.19 + 0.10x)m_0$ as an interpolation between bulk Si and Ge transverse masses and $m_z = 0.28m_0$.$\mu_L$ is the mobility due to bulk phonon scattering. In general, for $Si_{1-x}Ge_x$ binary alloy, the electron mobility $\mu_{L(SiGe)}^n = 1800 cm^2/V{\cdot}s$ and $\xi = 2.5$, the hole mobility $\mu_{L(SiGe)}^p = 700 cm^2/V{\cdot}s$ and $\xi = 2.2$.

Combining the Eq. (13) and Eq. (14), the electron and hole collision frequency can be expressed as

$$\begin{cases} \nu_n = \frac{e}{m_{cn}}\frac{1}{\mu_n} = \frac{e}{m_{cn}}\left[\frac{\left(V_{alloy}^n\right)^2 x(1-x)[n(l,d)]^{1/3}T^{1/2}}{K} + (\mu_{L(SiGe)}^n)^{-1}(\frac{T}{300})^{2.5} + \frac{1}{\mu_{np}}\right] \\ \nu_p = \frac{e}{m_{cp}}\frac{1}{\mu_p} = \frac{e}{m_{cp}}\left[\frac{\left(V_{alloy}^p\right)^2 x(1-x)[n(l,d)]^{1/3}T^{1/2}}{K} + (\mu_{L(SiGe)}^p)^{-1}(\frac{T}{300})^{2.2} + \frac{1}{\mu_{np}}\right] \end{cases} \tag{18}$$

where $V_{alloy}^n$ and $V_{alloy}^p$ denote the electron and hole alloy potential, respectively. $\mu_{L(SiGe)}^n$ and $\mu_{L(SiGe)}^p$ is the electron and hole mobility due to bulk phonon scattering. $\nu_n$ and $\nu_p$ are the collision frequency of the electrons and holes with other particles, respectively. Therefore, the total collision frequency is the linear combination of the electrons and holes collision frequency, which can be obtained as:

$$\begin{aligned} \nu = & \frac{e}{m_{cn(SiGe)}}\left[(V_{alloy}^n)^2 + (\mu_{L(SiGe)}^n)^{-1}\left(\frac{T}{300}\right)^{2.5}\right] \\ & + \frac{e}{m_{cp(SiGe)}}\left[(V_{alloy}^p)^2 + (\mu_{L(SiGe)}^p)^{-1}\left(\frac{T}{300}\right)^{2.2}\right] \\ & + \left(\frac{e}{m_{cn(SiGe)}} + \frac{e}{m_{cp(SiGe)}}\right)\left[\frac{x(1-x)[n(l,d)]^{1/3}T^{1/2}}{K}\right] \\ & + \left(\frac{e}{m_{cn(SiGe)}} + \frac{e}{m_{cp(SiGe)}} - \frac{e}{m_{c(SiGe)}}\right) \times \\ & \left[\frac{n(l,d)}{D(T/300)^{3/2}n(l,d)}\left(\ln\left(1 + F\left(\frac{T}{300}\right)^2 [n(l,d)]^{-2/3}\right)\right)\right] \end{aligned} \tag{19}$$

where

$$K = \frac{16e\hbar^3}{3m_{xy}^2\Omega_0 S(a)}\left(\frac{33m_z e^2}{8\varepsilon_{SiGe}\hbar^2}\right)^{-1/3}$$

$$m_{cn(Si_{1-x}Ge_x)} = (0.26 - 0.14x)m_0$$

$$m_{cp(Si_{1-x}Ge_x)} = (0.29 - 0.19x)m_0$$

$$m_{c(Si_{1-x}Ge_x)} = (1/m_{cn(Si_{1-x}Ge_x)} + 1/m_{cp(Si_{1-x}Ge_x)})^{-1}$$

where $m_{cn(Si_{1-x}Ge_x)}$ and $m_{cp(Si_{1-x}Ge_x)}$ is conductivity effective mass of the electron and hole, $m_{c(Si_{1-x}Ge_x)}$ is the reduced conductivity effective mass of electrons and holes. $n(l,d)$ is the two dimensional solid state plasma concentration distribution model within the I-region, as shown in Eq. (10).

## 4. Results and discussion

### 4.1. Correlation parameter and collision frequency simulation

To predict the trend of the collision frequency for different parameters, the Matlab's scripts were used. The length and depth of the I-region is L=100 μm, D=80 μm. Alloy scattering mobility for different Ge mole fraction x is shown in Fig. 3. At around room temperature, the mobility of the alloy scattering for electrons and holes will increase with the increasing Ge mole fraction x. The comparison of the model and published literature [18] result is presented and good agreements are clearly observed.

In the on state, when the excess solid state plasma concentration exceeds the base doping level by several orders of magnitude, carrier-carrier scattering can not be overlooked. Fig. 4 illustrates the calculated 2D mobility distribution of the carrier-carrier scattering within the I-

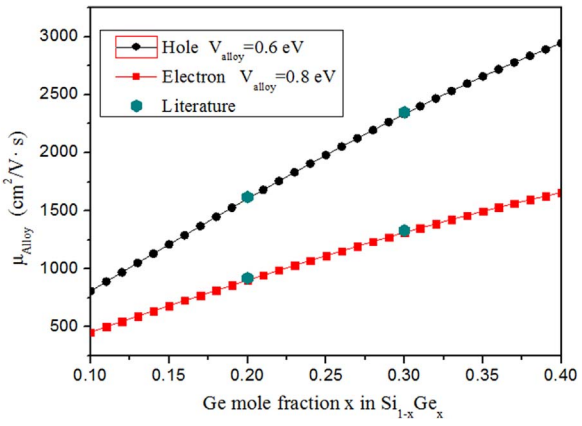


**Fig. 3.** The alloy scattering mobility versus Ge mole fraction x.

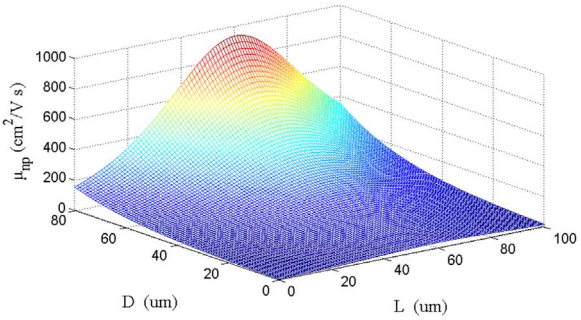


**Fig. 4.** 2D mobility distribution of the carrier-carrier scattering in the I-region.

region of the $Si/Si_{1-x}Ge_x/Si$ SPiN device at the room temperature T=300 K. Compared to the 2D plasma concentration distribution, it can be shown that the area where the solid state plasma concentration is higher, the mobility is relatively lower.

Fig. 5(a) and (b) illustrate the transverse and longitudinal concentration distribution of the solid state plasma for different Ge mole fraction x in the I-region of the SPiN device. This indicates that the slope of the plasma concentration is smaller at the Ni junction side when compared with the Pi junction side. The figure also show that the improvement in solid state plasma concentration with the increasing Ge mole fraction x. That is because the barrier height at the Pi/Ni heterojunction interface decreased, meanwhile, the band gap discontinuity in heterojunction obtained high injection ratio. Here the applied voltage is kept constant V=1 V. 2D solid state plasma concentration distribution within the I-region for Ge mole fraction x=0.1 and x=0.3 are displayed in Fig. 5(c). It can be seen that the solid state plasma concentration for x=0.3 is higher than that of x=0.1.

The 2D collision frequency distribution of the proposed model for the solid state plasma within the I-region for different Ge mole fraction x (x=0.1, x=0.3) at the same applied voltage V=1 V have been presented in Fig. 6a and Fig. 6(b). Compared the Fig. 5(c) to the Fig. 6, it is observed that, first, the 2D distribution of collision frequency and concentration for the solid state plasma within the I-region showed exactly the opposite trend. Second, it also displays that the values of the collision frequency for Ge mole fraction x=0.3 is lower than that of x=0.1. This reduction in the collision frequency with an increasing x can be attributed to a decreased built-in potential barrier potential and conductivity effective mass, then an increase the electrons and holes mobility, so a decreased collision frequency. Third, the distribution of the collision frequency for x=0.3 is basically uniform.

The extreme value of the collision frequency for Ge mole fraction x ($0 < x < 0.5$) is shown in Fig. 7(a). Both the maximum and minimum value decrease with the increasing Ge mole fraction x, however, the difference between them firstly decreased, and then increased with the Ge mole fraction x increase, which is displayed in Fig. 7(b). When the Ge mole fraction x increase, the conductivity effective mass of the electrons and holes will decrease, the plasma concentration of the I-region will increase due to the decreasing of the barrier potential. The difference δ will reach the minimum value at x=0.3, that means collision frequency is basically uniform distribution in the I-region considering the above two effects in combination.

The collision frequency of the proposed model for different applied

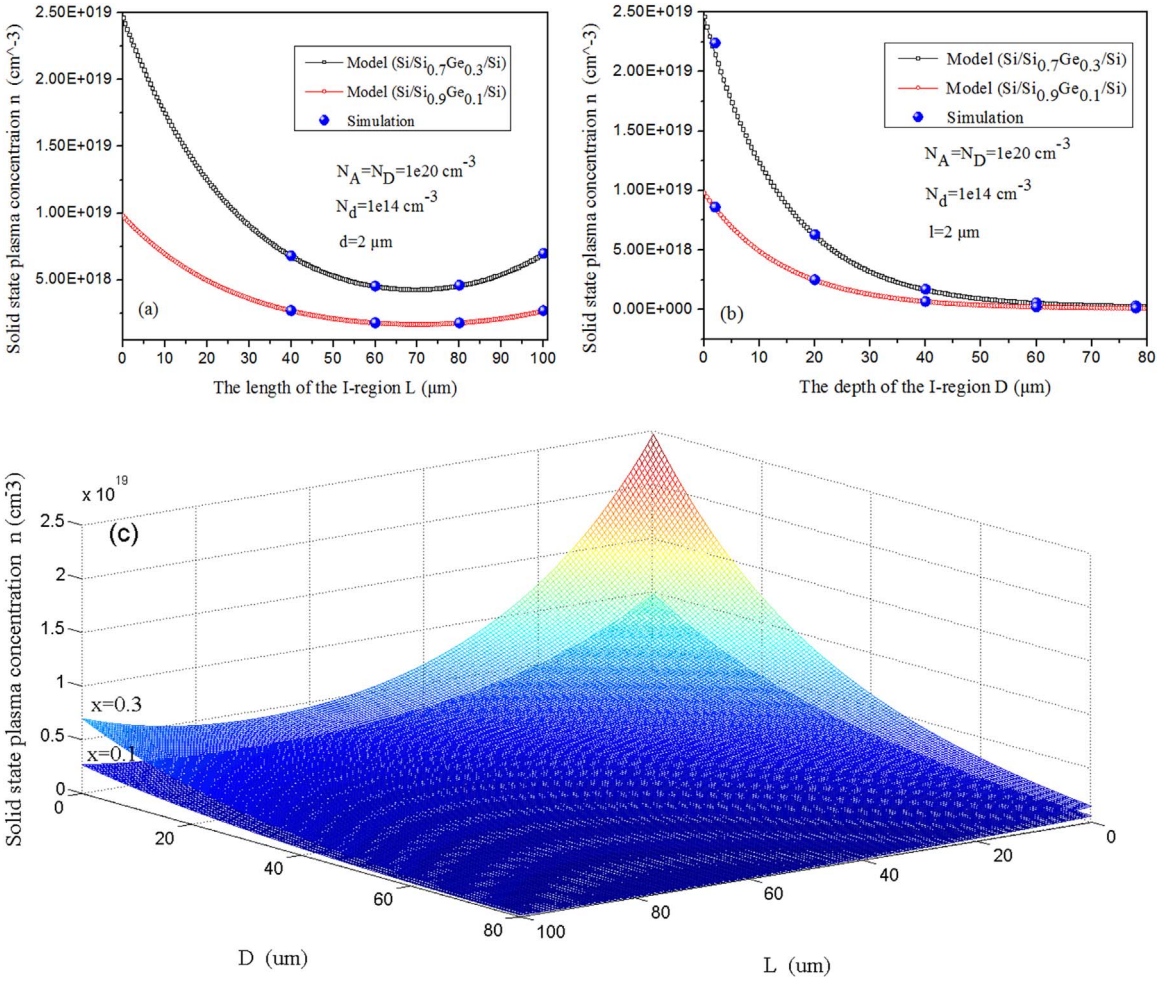


**Fig. 5.** Transverse concentration distribution (a), longitudinal concentration distribution (b) and two dimensional concentration distribution (c) in the I-region.

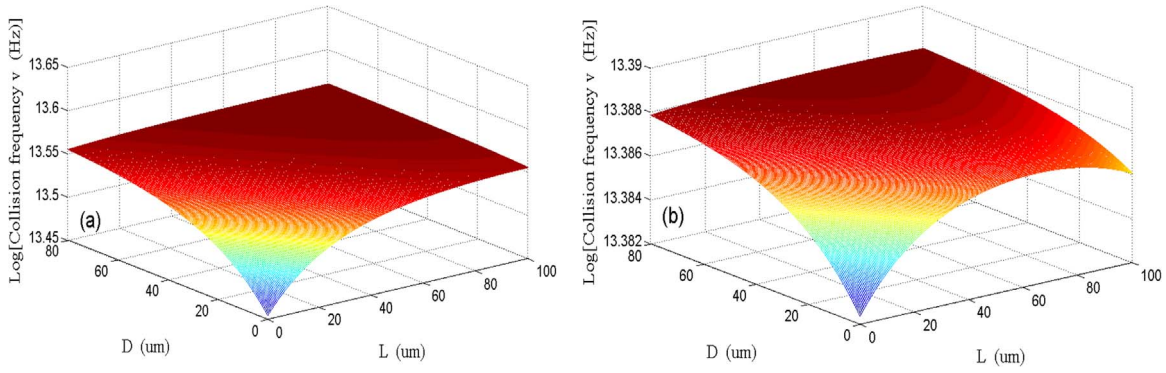


**Fig. 6.** Collision frequency for Ge x=0.1(a), Ge x=0.3 (b).

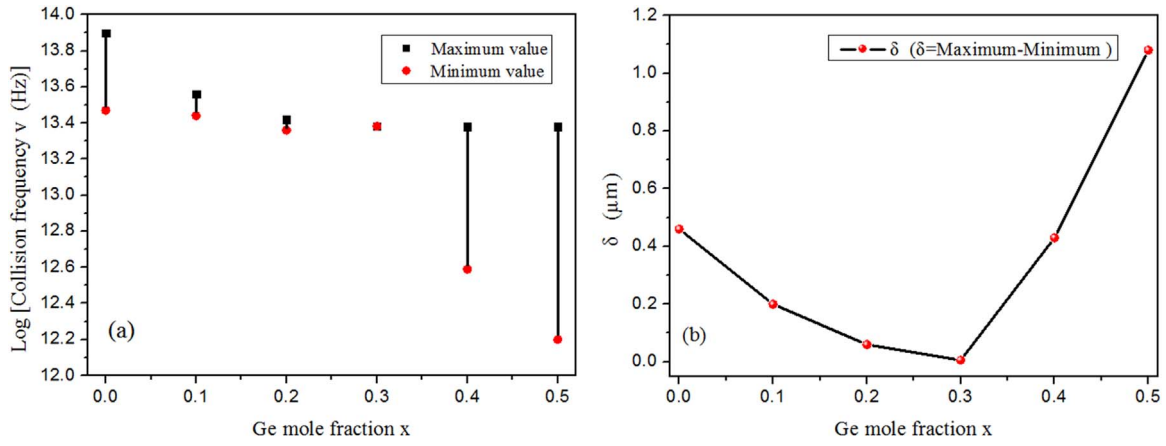


**Fig. 7.** The extreme value (a) and the difference (b) of collision frequency versus Ge mole fraction x.

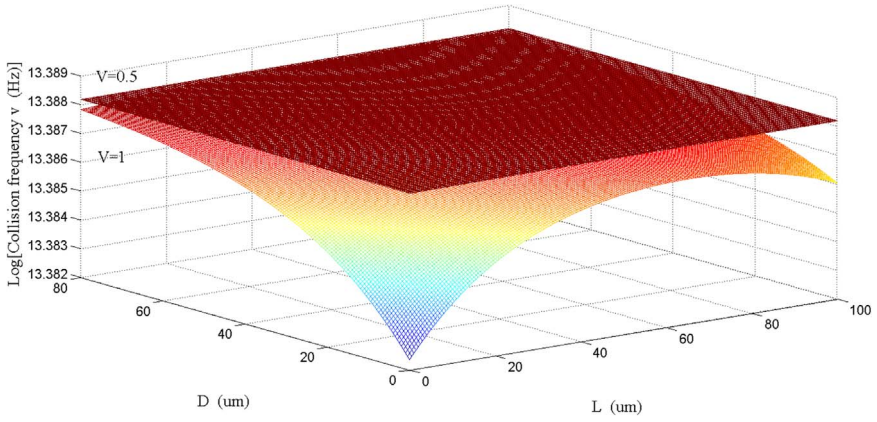


**Fig. 8.** Collision frequency of the proposed model for different applied voltage (V=0.5 V, V=1 V).

voltage is shown in Fig. 8. The results show that the values of the collision frequency for V=1 V is lower than that of V=0.5 V at both the Ge mole fraction x=0.3, that is because that the mobility is proportional to the applied voltage due to the electric field in the I-region is constant, so the collision frequency decrease. But on the other hand, the concentration will increase with the increasing applied voltage, which result in decreasing of the mobility for the carrier-carrier scattering, resulting in the collision frequency improve. Considering a reasonable tradeoff, the increased trend of mobility is greater than the downward trend. Therefore, the collision frequency will decrease when the applied voltage improve.

The 2D collision frequency distribution of solid state plasma within the I-region for different temperature (T=300 K, T=400 K) as shown in Fig. 9 at a constant Ge mole fraction x=0.3 and applied voltage V=1 V. It is clearly evident that the the collision frequency at the T=400 K is higher than that of T=300 K. This is mainly because that the increasing temperature enhance the movement of the carriers and shorten the mean free time, therefore, the collision frequency improve.

### 4.2. Effects of the collision frequency on the performance of plasma dipole antenna

In this paper, solid state plasma dipole antenna which is fabricated by the $Si/Si_{1-x}Ge_x/Si$ SPiN devices have been designed to verify the effects of the collision frequency on the performance of the antenna. The frequency of dipole antenna is f=10 GHz. Radiation efficiency and the maximum gain of the solid state plasma dipole antenna simulated with different collision frequency are calculated by HFSS are shown in Fig. 10(a) to Fig. 10(b). The results show that the radiation efficiency and maximum gain of the antenna is better if the collision frequency is

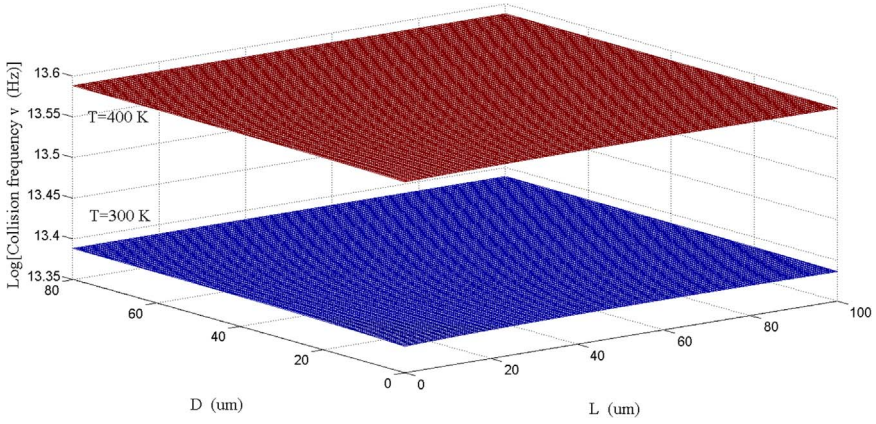


**Fig. 9.** Collision frequency of the proposed model for different temperature (T=300 K, T=400 K).

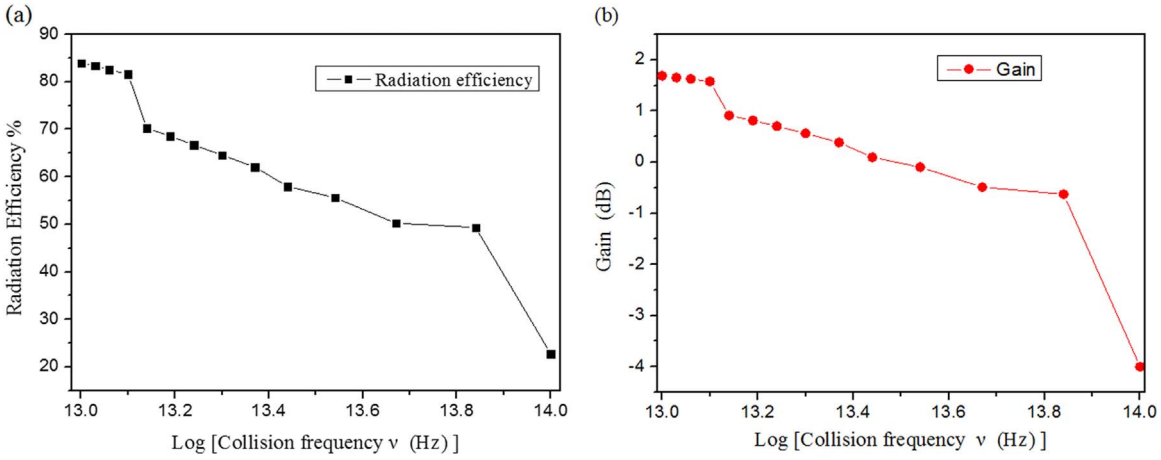


**Fig. 10.** The radiation efficiency (a) and maximum gain (b) versus collision frequency.

lower.

As the nonuniform distribution of the collision frequency in the I-region, simulated and actual values must have a large error. Therefore, through the above analysis, it can be summarized that the Ge mole fraction x=0.3 can be chosen to obtain the uniform collision frequency distribution. Consequently, improved performance of the solid state plasma antenna can be obtained by careful choice the heterojunction $Si/Si_{0.7}Ge_{0.3}/Si$ SPiN diode device as the basic radiating elements at the applied voltage V=1 V and the temperature T=300 K.

## 5. Conclusions

The 2D collision frequency model of the solid state plasma for the $Si/Si_{1-x}Ge_x/Si$ SPiN device have been developed based on the 2D solid state plasma concentration distribution model and mobility models within the I-region. It is clearly evident that the collision frequency of the solid state plasma will decrease with the increasing Ge mole fraction x($x < 0.5$) and the applied voltage. However, the collision frequency at the T=300 K will be lower than that of T=400 K. Moreover, the collision frequency of the solid state plasma shows a reverse trend to the concentration within the I-region. However, the basically uniform distribution of collision frequency can be obtained for Ge mole fraction x=0.3. Furthermore, the radiation efficiency and the maximum gain of the antenna are markedly affected by the collision frequency. Ultimately, the improved solid state plasma antenna can be obtained by using the heterojunction $Si/Si_{0.7}Ge_{0.3}/Si$ SPiN device as the basic radiation elements at the applied voltage V=1 V and the temperature T=300 K.

## Acknowledgements

This work has been supported by the National Natural Science Foundation of China (Grant No. 61474085). The authors would like to thank Professor Huiyong Hu for his many helpful discussions.

## References

[1] A.E. Fathy, A. Rosen, H.S. Owen, F. McGinty, D.J. McGee, G.C. Taylor, P.K. Swain, S.M. Perlow, M. ElSherbiny, IEEE Trans. Microwave Theory Tech. **51** (2003) 1650.
[2] Y.C. Zhai, Q. Wu, J.J. Tan, H. Tao, X.L. Huang, F.H. Gao, Z.Y. Zhang, J.L. Du, Y.D. Hou, Microelectron. Eng. **145** (2015) 49–52.
[3] Y. Yashchyshyn, J.W. Modelski, K. Derzakowski, P.B. Grabiec, IEEE Trans. Antennas Propag. **57** (2009) 2.
[4] R.P. Jackson, S.J.N. Mitchell, V. Fusco, Solid-State Electron. **54** (2010) 149.
[5] C. Wang, H.M. Zhang, J.J. Song, H.Y. Hu, SCI. China Phys. Mech. Astron. **54** (2011) 1801.
[6] C.W. Leitz, M.T. Currie, M.L. Lee, Z.Y. Cheng, D.A. Antoniadis, E.A. Fitzgerald, J. Appl. Phys. **92** (2002) 3745.
[7] Z.F. Di, Y.Q. Wang, M. Nastasi, G. Bisognin, M. Berti, P.E. Thompson, Appl. Phys. Lett. **94** (2009) 264102.
[8] S. Riyopoulos, Phys. Plasmas **12** (2005) 0707041.
[9] Z.S. Chen, J.M. Shi, L. Cheng, In: Proceedings of the 2015 7th International Conference on Intelligent Human-Machine Systems and Cybernetics (IHMSC), 2015, pp. 521
[10] F. Murphy-Armando, S. Fahy, J. Appl. Phys. **110** (2011) 1237061.
[11] Baliga BJayant. Fundamentals of power semiconductor devices, Carolina: English; 2008.
[12] A. Nusobaum, Solid-State Electron. 18 (1975) 107.
[13] E. K. Liu, Semiconductor Physics, Beijing, China, 2011.
[14] C. Lombardi, S. Manzini, A. Saporito, M. Vanzi, IEEE Trans. Comput.-Aided Des. Integr. Circuits Syst. **7** (1988) 1164.
[15] O. Bonno, J.L. Thobel, J. Appl. Phys. **104** (2008) 053719.
[16] V. Venkataraman, C.W. Liu, J.C. Sturm, Appl. Phys. Lett. 63 (1993) 2795.
[17] G. Masetti, M. Severi, S. Solmi, IEEE Trans. Electron Devices ED (1983) 764.
[18] S. Joyce, F. Murphy-Armando, S. Fahy, Phys. Rev. B 75 (2007) 1552011.